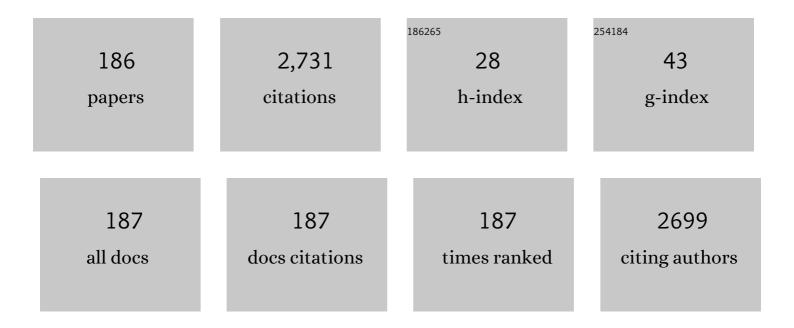
List of Publications by Year in descending order

Source: https://exaly.com/author-pdf/8506411/publications.pdf Version: 2024-02-01



СИЦ-НИЦ САЦ

#	Article	IF	CITATIONS
1	Undersampled MRI reconstruction with patch-based directional wavelets. Magnetic Resonance Imaging, 2012, 30, 964-977.	1.8	196
2	Iterative thresholding compressed sensing MRI based on contourlet transform. Inverse Problems in Science and Engineering, 2010, 18, 737-758.	1.2	131
3	Phase transformation mechanism between \hat{I}_{3-} and \hat{I}_{3-} alumina. Physical Review B, 2003, 67, .	3.2	81
4	Identification of biochemical changes in lactovegetarian urine using 1H NMR spectroscopy and pattern recognition. Analytical and Bioanalytical Chemistry, 2010, 396, 1451-1463.	3.7	77
5	Investigation of the contribution of total creatine to the CEST <i>Z</i> â€spectrum of brain using a knockout mouse model. NMR in Biomedicine, 2017, 30, e3834.	2.8	64
6	Adsorption of alcohols on \hat{I}^3 -alumina (1 1 0 C). Journal of Molecular Catalysis A, 2003, 193, 157-164.	4.8	62
7	Singleâ€shot T ₂ mapping using overlappingâ€echo detachment planar imaging and a deep convolutional neural network. Magnetic Resonance in Medicine, 2018, 80, 2202-2214.	3.0	61
8	Metabolic responses of Haliotis diversicolor to Vibrio parahaemolyticus infection. Fish and Shellfish Immunology, 2017, 60, 265-274.	3.6	55
9	Porous gold nanocluster-decorated manganese monoxide nanocomposites for microenvironment-activatable MR/photoacoustic/CT tumor imaging. Nanoscale, 2018, 10, 3631-3638.	5.6	54
10	NMR-based metabolomic analysis of Haliotis diversicolor exposed to thermal and hypoxic stresses. Science of the Total Environment, 2016, 545-546, 280-288.	8.0	51
11	Protein aggregation linked to Alzheimer's disease revealed by saturation transfer MRI. NeuroImage, 2019, 188, 380-390.	4.2	50
12	Atomic Scale Mechanism of the Transformation ofγ-Alumina toÎ,-Alumina. Physical Review Letters, 2002, 89, 235501.	7.8	45
13	Altered brain iron content and deposition rate in Huntington's disease as indicated by quantitative susceptibility MRI. Journal of Neuroscience Research, 2019, 97, 467-479.	2.9	45
14	Observation of true and pseudo NOE signals using CESTâ€MRI and CESTâ€MRS sequences with and without lipid suppression. Magnetic Resonance in Medicine, 2015, 73, 1615-1622.	3.0	43
15	Partial Fourier transform reconstruction for singleâ€shot MRI with linear frequencyâ€swept excitation. Magnetic Resonance in Medicine, 2013, 69, 1326-1336.	3.0	42
16	A simulation algorithm based on Bloch equations and product operator matrix: application to dipolar and scalar couplings. Journal of Magnetic Resonance, 2005, 172, 242-253.	2.1	40
17	Metabonomics studies of intact hepatic and renal cortical tissues from diabetic db/db mice using high-resolution magic-angle spinning 1H NMR spectroscopy. Analytical and Bioanalytical Chemistry, 2009, 393, 1657-1668.	3.7	40
18	Reconstruction of Self-Sparse 2D NMR Spectra from Undersampled Data in the Indirect Dimension. Sensors, 2011, 11, 8888-8909.	3.8	39

#	Article	IF	CITATIONS
19	Fast acquisition of high-resolution NMR spectra in inhomogeneous fields via intermolecular double-quantum coherences. Journal of Chemical Physics, 2009, 130, 084504.	3.0	35
20	An efficient de-convolution reconstruction method for spatiotemporal-encoding single-scan 2D MRI. Journal of Magnetic Resonance, 2013, 228, 136-147.	2.1	35
21	Separating fast and slow exchange transfer and magnetization transfer using offâ€resonance variableâ€delay multipleâ€pulse (VDMP) MRI. Magnetic Resonance in Medicine, 2018, 80, 1568-1576.	3.0	34
22	High-Resolution 2D <i>J</i> -Resolved Spectroscopy in Inhomogeneous Fields with Two Scans. Journal of the American Chemical Society, 2011, 133, 7632-7635.	13.7	32
23	High-resolution intermolecular zero-quantum coherence spectroscopy under inhomogeneous fields with effective solvent suppression. Physical Chemistry Chemical Physics, 2007, 9, 6231.	2.8	31
24	SPROM – an efficient program for NMR/MRI simulations of inter- and intra-molecular multiple quantum coherences. Comptes Rendus Physique, 2008, 9, 119-126.	0.9	29
25	High-Resolution Two-Dimensional J-Resolved NMR Spectroscopy for Biological Systems. Biophysical Journal, 2014, 106, 2061-2070.	0.5	29
26	High-resolution NMR spectroscopy in inhomogeneous fields. Progress in Nuclear Magnetic Resonance Spectroscopy, 2015, 90-91, 1-31.	7.5	29
27	Metabolomic responses of Haliotis diversicolor to organotin compounds. Chemosphere, 2017, 168, 860-869.	8.2	29
28	Highâ€resolution creatine mapping of mouse brain at 11.7 T using nonâ€steadyâ€state chemical exchange saturation transfer. NMR in Biomedicine, 2019, 32, e4168.	2.8	29
29	Investigation on the complex of diperoxovanadate with 2-(2′-pyridyl)-imidazole. Journal of Inorganic Biochemistry, 2005, 99, 1945-1951.	3.5	28
30	An aliasing artifacts reducing approach with random undersampling for spatiotemporally encoded single-shot MRI. Journal of Magnetic Resonance, 2013, 237, 115-124.	2.1	28
31	Theoretical Investigation of19F NMR Chemical Shielding of Alkaline-Earth-Metal and Alkali-Metal Fluorides. Journal of Physical Chemistry A, 2002, 106, 1060-1066.	2.5	27
32	Intermolecular single-quantum coherence sequences for high-resolution NMR spectra in in inhomogeneous fields. Journal of Magnetic Resonance, 2010, 203, 100-107.	2.1	27
33	Ultrafast 2D COSY with constant-time phase-modulated spatial encoding. Journal of Magnetic Resonance, 2010, 204, 82-90.	2.1	27
34	Spatially encoded ultrafast high-resolution 2D homonuclear correlation spectroscopy in in inhomogeneous fields. Journal of Magnetic Resonance, 2013, 227, 39-45.	2.1	27
35	High-Resolution 1H NMR Spectroscopy of Fish Muscle, Eggs and Small Whole Fish via Hadamard-Encoded Intermolecular Multiple-Quantum Coherence. PLoS ONE, 2014, 9, e86422.	2.5	26
36	A high-resolution 2D J-resolved NMR detection technique for metabolite analyses of biological samples. Scientific Reports, 2015, 5, 8390.	3.3	25

Ѕни-Ниі Саі

#	Article	IF	CITATIONS
37	NMR and Theoretical Study on the Coordination and Solution Structures of the Interaction between Diperoxovanadate Complexes and Histidine-like Ligands. Inorganic Chemistry, 2005, 44, 6755-6762.	4.0	24
38	Robust Single-Shot T ₂ Mapping via Multiple Overlapping-Echo Acquisition and Deep Neural Network. IEEE Transactions on Medical Imaging, 2019, 38, 1801-1811.	8.9	23
39	NMR spectroelectrochemistry in studies of hydroquinone oxidation by polyaniline thin films. Electrochimica Acta, 2018, 273, 300-306.	5.2	22
40	Ab initio calculations of 19FNMR chemical shielding for alkali-metal fluorides1Projects 19605004, 29892166 supported by National Natural Science Foundation of China, Natural Science Foundation of Fujian Province.1. Chemical Physics Letters, 1999, 302, 73-76.	2.6	21
41	Spectroscopic studies on the interactions between a bioactive diperoxovanadate complex and pyridine. Spectrochimica Acta - Part A: Molecular and Biomolecular Spectroscopy, 2004, 60, 391-396.	3.9	21
42	Super-resolved enhancing and edge deghosting (SEED) for spatiotemporally encoded single-shot MRI. Medical Image Analysis, 2015, 23, 1-14.	11.6	21
43	High-resolution two-dimensional correlation spectroscopy in inhomogeneous fields: New application of intermolecular zero-quantum coherences. Journal of Chemical Physics, 2010, 132, 134507.	3.0	19
44	Metabolomic Profilings of Urine and Serum from High Fat-Fed Rats via 1H NMR Spectroscopy and Pattern Recognition. Applied Biochemistry and Biotechnology, 2013, 169, 1250-1261.	2.9	19
45	Brown adipose tissue mapping in rats with combined intermolecular doubleâ€quantum coherence and Dixon water–fat MRI. NMR in Biomedicine, 2013, 26, 1663-1671.	2.8	19
46	Reduced field-of-view imaging for single-shot MRI with an amplitude-modulated chirp pulse excitation and Fourier transform reconstruction. Magnetic Resonance Imaging, 2015, 33, 503-515.	1.8	19
47	Freshness assessment of intact fish via 2D 1H J-resolved NMR spectroscopy combined with pattern recognition methods. Sensors and Actuators B: Chemical, 2018, 255, 348-356.	7.8	19
48	Ultrafast acquisition of localized two-dimensional magnetic resonance correlated spectra of inhomogeneous biological tissues with resolution improvements. Chemical Physics Letters, 2013, 581, 96-102.	2.6	18
49	Single-Shot \${ext{T}}_{{2}}\$ Mapping Through OverLapping-Echo Detachment (OLED) Planar Imaging. IEEE Transactions on Biomedical Engineering, 2017, 64, 2450-2461.	4.2	18
50	General Two-Dimensional Absorption-Mode <i>J</i> -Resolved NMR Spectroscopy. Analytical Chemistry, 2017, 89, 12646-12651.	6.5	18
51	1 H NMR-based compositional identification of different powdered infant formulas. Food Chemistry, 2017, 230, 164-173.	8.2	17
52	Accurate measurements of small J coupling constants under inhomogeneous fields via intermolecular multiple-quantum coherences. Journal of Magnetic Resonance, 2008, 190, 298-306.	2.1	16
53	Theoretical study on19F magnetic shielding constants of some metal fluorides. Magnetic Resonance in Chemistry, 2003, 41, 902-907.	1.9	15
54	Ultrahigh-Resolution NMR Spectroscopy for Rapid Chemical and Biological Applications in Inhomogeneous Magnetic Fields. Analytical Chemistry, 2017, 89, 7115-7122.	6.5	15

Ѕни-Ниі Саі

#	Article	IF	CITATIONS
55	Tungsten Atoms and Clusters Adsorbed on the MgO(001) Surface:Â A Density Functional Study. Journal of Physical Chemistry B, 2000, 104, 11506-11514.	2.6	14
56	19F NMR chemical shielding for metal fluorides MF2 (M=Zn, Cd, Pb), MF3 (M=Al, Ga, In) and SnF4. Chemical Physics Letters, 2002, 362, 13-18.	2.6	14
57	Positive Contrast Imaging of SPIO Nanoparticles. Journal of Nanomaterials, 2012, 2012, 1-9.	2.7	14
58	Highâ€resolution NMR spectroscopy in inhomogeneous fields via Hadamardâ€encoded intermolecular doubleâ€quantum coherences. NMR in Biomedicine, 2012, 25, 1088-1094.	2.8	14
59	Imaging with referenceless distortion correction and flexible regions of interest using single-shot biaxial spatiotemporally encoded MRI. NeuroImage, 2015, 105, 93-111.	4.2	14
60	Changes in brain iron concentration after exposure to high-altitude hypoxia measured by quantitative susceptibility mapping. NeuroImage, 2017, 147, 488-499.	4.2	14
61	Theoretical formalism and experimental verification of line shapes of NMR intermolecular multiple-quantum coherence spectra. Journal of Chemical Physics, 2005, 123, 074317.	3.0	13
62	Multinuclear NMR spectroscopic and theoretical study on the interactions between diperoxovanadate complex and picoline-like ligands. Spectrochimica Acta - Part A: Molecular and Biomolecular Spectroscopy, 2006, 65, 616-622.	3.9	13
63	NMR-based metabonomic analysis of MnO-embedded iron oxide nanoparticles as potential dual-modal contrast agents. Journal of Nanoparticle Research, 2014, 16, 1.	1.9	13
64	Motionâ€ŧolerant diffusion mapping based on singleâ€shot overlappingâ€echo detachment (OLED) planar imaging. Magnetic Resonance in Medicine, 2018, 80, 200-210.	3.0	13
65	A simultaneous multiâ€slice T ₂ mapping framework based on overlappingâ€echo detachment planar imaging and deep learning reconstruction. Magnetic Resonance in Medicine, 2022, 87, 2239-2253.	3.0	13
66	Comparison of direct 13 C and indirect 1 H-[13 C] MR detection methods for the study of dynamic metabolic turnover in the human brain. Journal of Magnetic Resonance, 2017, 283, 33-44.	2.1	12
67	Fast chemical exchange saturation transfer imaging based on PROPELLER acquisition and deep neural network reconstruction. Magnetic Resonance in Medicine, 2020, 84, 3192-3205.	3.0	12
68	Possible Dual-Charge-Carrier Mechanism of Surface Conduction on Î ³ -Alumina. Journal of Physical Chemistry C, 2007, 111, 5506-5513.	3.1	11
69	An Intermolecular Single-Quantum Coherence Detection Scheme for High-Resolution Two-Dimensional <i>J</i> -resolved Spectroscopy in Inhomogeneous Fields. Applied Spectroscopy, 2010, 64, 235-240.	2.2	11
70	Finite difference simulation of diffusion behaviors under inter- and intra-molecular multiple-quantum coherences in liquid NMR. Chemical Physics Letters, 2005, 407, 438-443.	2.6	10
71	Fast high-resolution 2D NMR spectroscopy in inhomogeneous fields via Hadamard frequency encoding and spatial encoding. Chemical Physics Letters, 2013, 582, 148-153.	2.6	10
72	High-resolution heteronuclear multi-dimensional NMR spectroscopy in magnetic fields with unknown spatial variations. Journal of Magnetic Resonance, 2014, 242, 49-56.	2.1	10

#	Article	IF	CITATIONS
73	The electrochemical oxidation of hydroquinone and catechol through polyaniline and poly(aspartic) Tj ETQq1	. 0.784314 1.3	rgBT/Overloc
74	Referenceless distortion correction of gradient-echo echo-planar imaging under inhomogeneous magnetic fields based on a deep convolutional neural network. Computers in Biology and Medicine, 2018, 100, 230-238.	7.0	10
75	Formation and identification of pure intermolecular zero-quantum coherence signal in liquid NMR. Chemical Physics Letters, 2006, 421, 171-178.	2.6	9
76	Interactions of methane, ethane and pentane with the (110C) surface of Î ³ -alumina. Journal of Molecular Catalysis A, 2007, 275, 63-71.	4.8	9
77	Investigation on the complex of diperoxovanadate with picolinamide. Spectrochimica Acta - Part A: Molecular and Biomolecular Spectroscopy, 2009, 72, 965-969.	3.9	9
78	High-resolution NMR spectroscopy in inhomogeneous fields via heteronuclear intermolecular multiple-quantum coherences. Chemical Physics Letters, 2009, 471, 331-336.	2.6	9
79	High-resolution 2D NMR spectra in inhomogeneous fields based on intermolecular multiple-quantum coherences with efficient acquisition schemes. Journal of Magnetic Resonance, 2011, 208, 87-94.	2.1	9
80	Theoretical investigation on the band structures of several Chevrel-phase compounds. Journal of the Chemical Society, Faraday Transactions, 1995, 91, 479.	1.7	8
81	Studies on the band structures of some layered transition metal dichalcogenides. Computational and Theoretical Chemistry, 1996, 362, 379-385.	1.5	8
82	Double-quantum-filtered intermolecular single-quantum coherences in nuclear magnetic resonance spectroscopy and imaging. Chemical Physics Letters, 2006, 429, 611-616.	2.6	8
83	Spectroscopic and theoretical study on the interaction between diperoxovanadate and oxazole. Spectrochimica Acta - Part A: Molecular and Biomolecular Spectroscopy, 2008, 69, 117-122.	3.9	8
84	High-resolution NMR spectra in inhomogeneous fields utilizing the CRAZED sequence without coherence selection gradients. Journal of Magnetic Resonance, 2008, 193, 94-101.	2.1	8
85	High-resolution absorptive intermolecular multiple-quantum coherence NMR spectroscopy under inhomogeneous fields. Journal of Magnetic Resonance, 2012, 214, 289-295.	2.1	8
86	Spatially-encoded intermolecular single-quantum coherence method for high-resolution NMR spectra in inhomogeneous fields. Chemical Physics Letters, 2015, 634, 11-15.	2.6	8
87	Ultrafast multi-slice spatiotemporally encoded MRI with slice-selective dimension segmented. Journal of Magnetic Resonance, 2016, 269, 138-145.	2.1	8
88	NMR Spectroelectrochemistry in Studies of Dopamine Oxidation. Electrochemistry, 2020, 88, 200-204.	1.4	8
89	Suppression of undesired peaks due to residual intermolecular dipolar interactions in liquid NMR. Chemical Physics Letters, 2006, 417, 48-52.	2.6	7
90	Adsorption of 1-hexene on γ-alumina (110C). Journal of Molecular Catalysis A, 2006, 248, 76-83.	4.8	7

#	Article	IF	CITATIONS
91	NMR and theoretical study on interactions between diperoxovanadate complex and 4-substituted pyridines. Spectrochimica Acta - Part A: Molecular and Biomolecular Spectroscopy, 2008, 71, 644-649.	3.9	7
92	Intermolecular multiple-quantum coherences between spin 1/2 and quadrupolar nuclei in liquid nuclear magnetic resonance. Chemical Physics Letters, 2008, 458, 368-372.	2.6	7
93	Study on structural variation of oxalate-oxodiperoxovanadate(V) from solid state to solution using NMR spectroscopy and theoretical calculation. Inorganic Chemistry Communication, 2009, 12, 1259-1262.	3.9	7
94	Homonuclear decoupled proton NMR spectra in modest to severe inhomogeneous fields via distant dipolar interactions. Chemical Physics Letters, 2010, 492, 174-178.	2.6	7
95	Fast high-resolution 2D correlation spectroscopy in inhomogeneous fields via Hadamard intermolecular multiple quantum coherences technique. Journal of Magnetic Resonance, 2011, 211, 162-169.	2.1	7
96	Statistical two-dimensional correlation spectroscopy of urine and serum from metabolomics data. Chemometrics and Intelligent Laboratory Systems, 2012, 112, 33-40.	3.5	7
97	A fast chemical exchange saturation transfer imaging scheme based on single-shot spatiotemporal encoding. Magnetic Resonance in Medicine, 2017, 77, 1786-1796.	3.0	7
98	Ultrafast multi-slice chemical exchange saturation transfer imaging scheme based on segmented spatiotemporal encoding. Magnetic Resonance Imaging, 2019, 60, 122-129.	1.8	7
99	Valence-band offsets of III-V alloy heterojunctions. Surface and Interface Analysis, 1999, 28, 177-180.	1.8	6
100	Simultaneous acquisition and effective separation of intermolecular multiple-quantum signals of different orders. Chemical Physics Letters, 2007, 438, 308-314.	2.6	6
101	Intermolecular double-quantum coherence NMR spectroscopy in moderate inhomogeneous fields. Spectrochimica Acta - Part A: Molecular and Biomolecular Spectroscopy, 2009, 74, 1138-1144.	3.9	6
102	Synthesis and Spectroscopic Characterizations of an Insulinomimetic Peroxovanadate Complex in Aqueous Solution. Chinese Journal of Chemistry, 2003, 21, 746-750.	4.9	6
103	Spectroscopic and DFT Study on the Interaction System of Vanadium with <scp>l</scp> -Proline in Aqueous Solution. Journal of Physical Chemistry A, 2010, 114, 5211-5216.	2.5	6
104	High-resolution magnetic resonance spectroscopy in unstable fields via intermolecular zero-quantum coherences. Physical Chemistry Chemical Physics, 2010, 12, 6014.	2.8	6
105	Fast 3D gradient shimming by only 2×2 pixels in XY plane for NMR-solution samples. Journal of Magnetic Resonance, 2014, 248, 13-18.	2.1	6
106	High-resolution nuclear magnetic resonance measurements in inhomogeneous magnetic fields: A fast two-dimensional <i>J</i> -resolved experiment. Journal of Chemical Physics, 2016, 144, 104202.	3.0	6
107	Spatially Localized Two-Dimensional J-Resolved NMR Spectroscopy via Intermolecular Double-Quantum Coherences for Biological Samples at 7 T. PLoS ONE, 2015, 10, e0134109.	2.5	6
108	Ultrafast water–fat separation using deep learning–based singleâ€shot MRI. Magnetic Resonance in Medicine, 2022, 87, 2811-2825.	3.0	6

#	Article	IF	CITATIONS
109	Singleâ€shot T ₂ mapping via multiâ€echoâ€train multiple overlappingâ€echo detachment planar imaging and multitask deep learning. Medical Physics, 2022, 49, 7095-7107.	3.0	6
110	NMR studies on [VS4–Cun] (n=3, 4, 5, 6) clusters. Polyhedron, 1999, 18, 1339-1343.	2.2	5
111	Density functional model cluster study of adsorption of acetylene on magnesium oxide. Surface Science, 2001, 479, 169-182.	1.9	5
112	Investigation on the interactions between diperoxovanadate and substituted phenanthroline. Spectrochimica Acta - Part A: Molecular and Biomolecular Spectroscopy, 2006, 64, 255-263.	3.9	5
113	Apparent longitudinal relaxation in solutions with intermolecular dipolar interactions and slow chemical exchange. Chemical Physics Letters, 2007, 446, 223-227.	2.6	5
114	High-Resolution <i>J</i> -Scaling Nuclear Magnetic Resonance Spectra in Inhomogeneous Fields via Intermolecular Multiple-Quantum Coherences. Applied Spectroscopy, 2009, 63, 585-590.	2.2	5
115	Entropic Contributions to the Atomic-Scale Charge-Carrier/Surface Interactions That Govern Macroscopic Surface Conductance. Journal of Physical Chemistry C, 2010, 114, 3991-3997.	3.1	5
116	High-resolution NMR spectra in inhomogeneous and unstable fields via the three-pulse method. Molecular Physics, 2010, 108, 1869-1875.	1.7	5
117	Ultrafast localized twoâ€dimensional magnetic resonance correlated spectroscopy via spatially encoded technique. Magnetic Resonance in Medicine, 2014, 71, 903-910.	3.0	5
118	Discrete decoding based ultrafast multidimensional nuclear magnetic resonance spectroscopy. Journal of Chemical Physics, 2015, 143, 024201.	3.0	5
119	Ultrafast multidimensional nuclear magnetic resonance technique: A proof of concept based on inverse- <i>k</i> -space for convenient and efficient performance. Applied Physics Letters, 2016, 108, .	3.3	5
120	A 2D proton J-resolved NMR method for direct measurements on heterogeneous foods. Food Research International, 2016, 80, 70-77.	6.2	5
121	Selection of intra- or inter-molecular multiple-quantum coherences in NMR of highly polarized solution. Physica B: Condensed Matter, 2005, 362, 286-294.	2.7	4
122	Propagator formalism and computer simulation of restricted diffusion behaviors of inter-molecular multiple-quantum coherences. Physica B: Condensed Matter, 2005, 366, 127-137.	2.7	4
123	Advances in high-resolution nuclear magnetic resonance methods in inhomogeneous magnetic fields using intermolecular multiple quantum coherences. Science in China Series G: Physics, Mechanics and Astronomy, 2009, 52, 58-69.	0.2	4
124	Theoretical studies on the band structures of superconducting solid compounds: Nb ₃ X (X=Si, Ge, Sn, Pb). Chinese Journal of Chemistry, 1994, 12, 385-391.	4.9	4
125	Highly efficient square wave distant dipolar field and its application for in vivo MRI. Magnetic Resonance in Medicine, 2010, 64, 1128-1134.	3.0	4
126	Multinuclear nuclear magnetic resonance and density functional theoretical studies on the structure of bisperoxovanadium complexes with bidentate donors. Inorganica Chimica Acta, 2011, 365, 119-126.	2.4	4

#	Article	IF	CITATIONS
127	Intermolecular Zero Quantum Coherence in NMR Spectroscopy. Annual Reports on NMR Spectroscopy, 2013, 78, 209-257.	1.5	4
128	Hadamard-encoded high-resolution NMR spectroscopy via intermolecular single-quantum coherences. Chemical Physics, 2014, 444, 61-65.	1.9	4
129	Accelerating two-dimensional nuclear magnetic resonance correlation spectroscopy via selective coherence transfer. Journal of Chemical Physics, 2017, 146, 014202.	3.0	4
130	Studies on the band structures of some Laves-phase compounds. Polyhedron, 1995, 14, 3537-3544.	2.2	3
131	Storage capacity of the Hopfield neural network. Physica A: Statistical Mechanics and Its Applications, 1997, 246, 313-319.	2.6	3
132	Chaos suppression by feedback control in nuclear magnetic resonance. Physica B: Condensed Matter, 2007, 396, 57-61.	2.7	3
133	Theoretical investigation on multinuclear NMR chemical shifts of some tris(trifluoromethyl)boron complexes. Magnetic Resonance in Chemistry, 2009, 47, 629-634.	1.9	3
134	Harmonic peaks in 1D NMR spectra induced by radiation damping fields. Chemical Physics Letters, 2009, 479, 165-170.	2.6	3
135	Observation and characterization of NMR signals in spin-1 system based on intermolecular multiple-quantum coherences. Chemical Physics Letters, 2009, 481, 130-136.	2.6	3
136	The structure, stability, and reactivity of oxalato-monoperoxovanadium(V) in solution. Journal of Coordination Chemistry, 2010, 63, 3268-3278.	2.2	3
137	A new solvent suppression method via radiation damping effect. Chinese Physics B, 2011, 20, 118201.	1.4	3
138	Accurate Measurement of Small J Couplings. Annual Reports on NMR Spectroscopy, 2011, , 157-183.	1.5	3
139	High-resolution NMR spectroscopy in unstable and inhomogeneous fields via stroboscopic acquisition. Spectrochimica Acta - Part A: Molecular and Biomolecular Spectroscopy, 2011, 79, 112-117.	3.9	3
140	In vivo spatially localized high resolution ¹ H MRS via intermolecular singleâ€quantum coherence of rat brain at 7 T. Journal of Magnetic Resonance Imaging, 2013, 37, 359-364.	3.4	3
141	Fast high-resolution J-resolved correlation spectroscopy in inhomogeneous fields. Chemical Physics Letters, 2014, 616-617, 199-204.	2.6	3
142	Chemical exchange saturation transfer MRI using intermolecular double-quantum coherences with multiple refocusing pulses. Magnetic Resonance Imaging, 2014, 32, 759-765.	1.8	3
143	Variable density sampling and non-Cartesian super-resolved reconstruction for spatiotemporally encoded single-shot MRI. Journal of Magnetic Resonance, 2016, 272, 1-9.	2.1	3
144	Fast quantitative susceptibility reconstruction via total field inversion with improved weighted L 0 norm approximation. NMR in Biomedicine, 2019, 32, e4067.	2.8	3

#	Article	IF	CITATIONS
145	A Single-Scan Inhomogeneity-Tolerant NMR Method for High-Resolution Two-Dimensional J-Resolved Spectroscopy. IEEE Transactions on Biomedical Engineering, 2019, 66, 1559-1566.	4.2	3
146	Revealing weak histidine 15N homonuclear scalar couplings using Solid-State Magic-Angle-Spinning NMR spectroscopy. Journal of Magnetic Resonance, 2020, 316, 106757.	2.1	3
147	Singleâ€step calculation of susceptibility through multiple orientation sampling. NMR in Biomedicine, 2021, 34, e4517.	2.8	3
148	Numerical Simulations of Contribution of Chemical Shift in Novel Magnetic Resonance Imaging. Lecture Notes in Computer Science, 2006, , 374-383.	1.3	3
149	High-Resolution Solution NMR Spectra in Inhomogeneous Magnetic Fields. Current Analytical Chemistry, 2009, 5, 70-83.	1.2	2
150	Detection and characterization of intermolecular multiple-quantum coherence NMR signals of IS (I=1/2; S=3/2) spin systems. Spectrochimica Acta - Part A: Molecular and Biomolecular Spectroscopy, 2011, 78, 1051-1057.	3.9	2
151	Hadamard encoded 2D correlation spectroscopy in inhomogeneous fields. Chemical Physics Letters, 2013, 563, 102-106.	2.6	2
152	Ultrafast 1H J-resolved spectroscopy via 2H distant dipolar field in magnetic fields with unknown spatial variations. Chemical Physics Letters, 2013, 587, 99-104.	2.6	2
153	A Novel Detection Scheme for High-Resolution Two-Dimensional Spin-Echo Correlated Spectra in Inhomogeneous Fields. PLoS ONE, 2014, 9, e84032.	2.5	2
154	Fast high-resolution nuclear magnetic resonance spectroscopy through indirect zero-quantum coherence detection in inhomogeneous fields. Chinese Physics B, 2014, 23, 063201.	1.4	2
155	HRJCOSY: A three-dimensional NMR method for measuring complex samples in inhomogeneous magnetic fields. Chemical Physics Letters, 2014, 609, 21-25.	2.6	2
156	Single-Scan High-Resolution 2-D \$J\$ -Resolved Spectroscopy in Inhomogeneous Magnetic Fields. IEEE Transactions on Biomedical Engineering, 2018, 65, 440-448.	4.2	2
157	Super-resolved water/fat image reconstruction based on single-shot spatiotemporally encoded MRI. Journal of Magnetic Resonance, 2020, 314, 106736.	2.1	2
158	Observation of intermolecular double-quantum coherence signal dips in nuclear magnetic resonance. Chinese Physics B, 2011, 20, 103301.	1.4	2
159	An average-bond-energy method used for band-offset calculation for a strained heterojunction. Journal of Physics Condensed Matter, 2000, 12, 7759-7770.	1.8	1
160	Application of the forward linear prediction on high-resolution NMR spectra in inhomogeneous fields. Spectrochimica Acta - Part A: Molecular and Biomolecular Spectroscopy, 2008, 71, 1027-1031.	3.9	1
161	Spectroscopic and theoretical study on the interaction between diperoxovanadate complexes and glycyl-histidine. Spectrochimica Acta - Part A: Molecular and Biomolecular Spectroscopy, 2010, 77, 825-831.	3.9	1
162	Multinuclear NMR and theoretical investigation on interactions between diperoxovanadate complex and 4-picoline-like ligands. Spectrochimica Acta - Part A: Molecular and Biomolecular Spectroscopy, 2010, 75, 83-87.	3.9	1

Sнu-Ниі Саі

#	Article	IF	CITATIONS
163	Apparent diffusion behaviors of spins in the presence of distant dipolar field in two-component solution NMR. Molecular Physics, 2011, 109, 1943-1952.	1.7	1
164	High-resolution MR spectroscopy via intermolecular double-quantum coherences in inhomogeneous B0 and B1 fields. Magnetic Resonance Imaging, 2011, 29, 601-607.	1.8	1
165	Flat pancake distant dipolar fields for enhancement of intermolecular multiple-quantum coherence signals. Journal of Chemical Physics, 2012, 136, 094503.	3.0	1
166	Intermolecular double-quantum coherence imaging without coherence selection gradients and its application in in vivo MRI. Magnetic Resonance Imaging, 2013, 31, 515-523.	1.8	1
167	Establishing resolution-improved NMR spectroscopy in high magnetic fields with unknown spatiotemporal variations. Journal of Chemical Physics, 2015, 143, 244201.	3.0	1
168	Flexible reduced field of view magnetic resonance imaging based on single-shot spatiotemporally encoded technique. Chinese Physics B, 2015, 24, 108703.	1.4	1
169	Hadamard-encoded localized high-resolution NMR spectroscopy via intermolecular double-quantum coherences. Chemical Physics Letters, 2015, 622, 63-68.	2.6	1
170	Rapid reconstruction of quantitative susceptibility mapping via improved <mml:math xmlns:mml="http://www.w3.org/1998/Math/MathML" altimg="si0057.gif" overflow="scroll"> <mml:msub> <mml:mrow> <mml:mo>â,," </mml:mo> </mml:mrow> <mml:mrow> <mml:mn>0 <!--<br-->approximation. Computers in Biology and Medicine, 2016, 79, 59-67.</mml:mn></mml:mrow></mml:msub></mml:math 	710 mml:mn>	
171	A heteronuclear intermolecular single-quantum coherence scheme for high-resolution 2D <i>J</i> -resolved ¹ H NMR spectra in inhomogeneous magnetic fields. Molecular Physics, 2016, 114, 1520-1527.	1.7	1
172	A method for longitudinal relaxation time measurement in inhomogeneous fields. Journal of Magnetic Resonance, 2017, 281, 118-124.	2.1	1
173	Weighted total variation using split Bregman fast quantitative susceptibility mapping reconstruction method. Chinese Physics B, 2018, 27, 088701.	1.4	1
174	Accelerating multi-slice spatiotemporally encoded MRI with simultaneous echo refocusing. Journal of Magnetic Resonance, 2018, 296, 12-22.	2.1	1
175	High-resolution two-dimensional 1H J-resolved MRS measurements on in vivo samples. Journal of Magnetic Resonance, 2019, 300, 51-60.	2.1	1
176	Boosting C3-alcohol electrooxidations by co-fueling with formic acid: A real-time quantitative nuclear magnetic resonance spectroelectrochemical study. Journal of Catalysis, 2021, 404, 551-559.	6.2	1
177	Studies on the band structures of some low-temperature superconductors. International Journal of Quantum Chemistry, 1997, 64, 459-472.	2.0	Ο
178	Migration of Aluminum Atoms in the Transformation of γ–to Î,–Alumina. Materials Research Society Symposia Proceedings, 2002, 731, 361.	0.1	0
179	Modeling and simulation of magnetic resonance imaging based on intermolecular multiple quantum coherences. , 2006, , .		0
180	Crystal structure of ammonium (picolinamide)oxodiperoxovanadate(V) monohydrate, NH4[VO(O2)2(C6H6N2O)] ·H2O. Zeitschrift Fur Kristallographie - New Crystal Structures, 2008, 223, 449-450.	0.3	0

#	Article	IF	CITATIONS
181	Signal Reconstruction in Unstable Magnetic Field NMR with Wavelet Analysis. , 2009, , .		Ο
182	1H NMR-Based Metabonomics Study of Urine and Serum Samples from Diabetic db/db Mice. , 2009, , .		0
183	<i>Ab Initio</i> calculation of ¹⁹ F NMR chemical shielding for alkalineâ€earthâ€metal fluorides. Chinese Journal of Chemistry, 2001, 19, 1179-1183.	4.9	Ο
184	Localised two-dimensional correlated spectroscopy based on Hadamard encoding technique. Molecular Physics, 2014, 112, 2602-2607.	1.7	0
185	High-resolution heteronuclear correlation spectroscopy based on spatial encoding and coherence transfer in inhomogeneous fields. Molecular Physics, 2015, 113, 3353-3361.	1.7	Ο
186	Super-resolved reconstruction method for spatiotemporally encoded magnetic resonance imaging based on deep neural network. Wuli Xuebao/Acta Physica Sinica, 2022, 71, 058702.	0.5	0